Role of scalar dibaryon and $f_0(500)$ in the isovector channel of low-energy neutron-proton scattering

Werner Deinet,[1] Khaled Teilab,[1,2] Francesco Giacosa,[1,3] and Dirk H. Rischke[1]

[1]*Goethe University Frankfurt am Main, Institute for Theoretical Physics, Max-von-Laue-Straße 1, D-60438 Frankfurt am Main, Germany*

[2]*Faculty of Science, Cairo University, 12613 Giza, Egypt*

[3]*Institute of Physics, Jan Kochanowski University, ul. Swietokrzyska 15, 25-406 Kielce, Poland*

(Received 20 March 2016; published 31 October 2016)

We calculate the total and the differential cross section for np scattering at low energies in the isospin $I = 1$ channel within the so-called extended linear sigma model. This model contains conventional (pseudo)scalar and (axial-)vector mesons, as well as the nucleon and its chiral partner within the mirror assignment. In order to obtain good agreement with experimental data analysis results we need to consider two additional resonances: the lightest scalar state $f_0(500)$ and a dibaryon state with quantum numbers $I = 1$, $J^P = 0^+$ (also known as ${}^1S_0$ resonance). The resonance $f_0(500)$ is coupled to nucleons in a chirally invariant way through the mirror assignment and is crucial for a qualitatively correct description of the shape of the differential cross section. On the other hand, the dibaryon is exchanged in the s channel and is responsible of the large cross section close to threshold. We compare our results to data analysis results performed by the SAID program of the CNS Data Analysis Center (in the following "SAID results").

DOI: 10.1103/PhysRevC.94.044001

I. INTRODUCTION

Nucleon-nucleon scattering at low energies has been investigated using different effective approaches (see, e.g., Refs. [1–13]) which are constructed according to the principles of chiral perturbation theory (ChPT) [14] (see also Ref. [15] and references therein), the low-energy effective theory of the theory of strong interactions, quantum chromodynamics (QCD). In ChPT, the chiral symmetry of QCD is nonlinearly realized.

As initiated long ago in Ref. [16] (see also Ref. [17]), another possibility to describe low-energy hadronic physics is based on the linear realization of chiral symmetry via so-called linear sSigma models; see, e.g., Ref. [18]. A modern variant is the extended linear sigma model (eLSM), which contains (pseudo)scalar and (axial-)vector mesons and which was successfully applied in the context of meson-meson interactions [19–22] and also meson-nucleon interactions [23–25]. In particular, baryons and their chiral partners are treated in the so-called mirror assignment, in which a chirally invariant mass term is present [26–28]. This is important, since the smallness of the πN sigma term implies that chiral symmetry breaking alone cannot be responsible for the nucleon mass and other sources (such as a gluon condensate) must exist which contribute to generating the mass of the nucleon.

In this work, we use the eLSM in order to study nucleon-nucleon scattering. In particular, we investigate neutron-proton scattering in the $I = 1$ channel up to a nucleon momentum of about 0.4 GeV in the center-of-momentum (c.m.) frame. In order to describe experimental data analysis results, we need, apart from the usual quark-antiquark fields (see, e.g., Ref. [29]), to also incorporate the light $f_0(500)$ meson (for studies of this resonance see, e.g., Refs. [30,31] as well as the recent review [32]). As first shown in Ref. [23] and then further investigated in Refs. [33,34], the resonance $f_0(500)$ can be coupled to the eLSM in a chirally invariant way; the condensation of the field associated with this resonance is then responsible for the emergence of the chirally invariant mass term mentioned above. As shown in Ref. [33] by studying nuclear matter saturation and in Ref. [35] by studying the binding energy of nuclei, this resonance generates an attraction between nucleons. In the present work we will confirm that its coupling to nucleons is necessary for a reasonable description of neutron-proton scattering data.

However, the exchange of mesons alone (even after the inclusion of $f_0(500)$) is *not* capable of describing the enhanced interaction close to the neutron-proton threshold. As discussed previously in Ref. [2], an additional resonance with baryon number 2, isospin 1, as well as $J^P = 0^+$ (equivalent to ${}^1S_0$ in the old spectroscopic notation) can be introduced to effectively describe neutron-proton scattering. Namely, this dibaryon resonance (sometimes called "dimeron" [10]) is exchanged in the s channel and enhances considerably the cross section at threshold (up to a nucleon c.m. momentum p of about 0.2 GeV). We will also determine the parameters of this resonance, such as the nominal mass m_R and width and, more importantly, we will investigate the existence of a pole in the complex $\sqrt{s}$ plane and estimate its position. It turns out that the on-shell tree-level decay width is larger than the difference $D_R \equiv m_R - m_p - m_n$ of its mass from the threshold. As a consequence, this state is not a conventional Breit-Wigner resonance due to strong threshold effects.

Indeed, in some of the previous works [8,9,11] the dibaryon field was regarded as an auxiliary field that can be integrated out in order to obtain an effective Lagrangian which contains only nucleonic degrees of freedom. For the purpose of nucleon-nucleon scattering phenomenology, this is certainly a reasonable and well-defined approach. However, we believe that it is interesting to treat this state as a dibaryon resonance. Moreover, as a consequence, we also expect an analogous resonance in the neutron-neutron channel and possibly also in the proton-proton channel.

This paper is organized as follows: in Sec. II we present the model with special attention to the resonance $f_0(500)$ and the dibaryon resonance. In Sec. III we discuss our results for the $I = 1$ neutron-proton total and differential cross

sections, step by step including various contributions. The cross sections are compared to experimental data analysis results from the SAID program of the CNS Data Analysis Center[1] [36]. Finally, in Sec. IV we give our conclusions and an outlook.

II. THE MODEL

The Lagrangian of the model used in our calculations has three parts:

(i) The mesonic part of the eLSM Lagrangian. This has been developed and investigated for the two-flavor case ($N_f = 2$) in Refs. [19,20], for the three-flavor case ($N_f = 3$) in Refs. [21,22], and recently for the four-flavor case ($N_f = 4$) in Ref. [37]. For the explicit form of the Lagrangian, see the aforementioned references.

(ii) The nucleonic part of the eLSM Lagrangian. For $N_f = 2$, it includes the interaction of the nucleon and its chiral partner N^* (both states referred to as "nucleons" in the following) with $\bar{q}q$ mesons and a scalar isoscalar meson $f_0(500)$ [23,24,33] in a chirally invariant framework (recently, the baryonic Lagrangian has been extended to $N_f = 3$ in Ref. [25]). In Sec. II A we present the Lagrangian for $N_f = 2$ together with its parameters, while in Sec. II B we consider only those terms which enter the calculation of nucleon-nucleon scattering. Moreover, we also show how to include a form factor which suppresses the interaction strength at high momenta.

(iii) The Lagrangian describing the interactions of two nucleons with the ${}^1S_0$ dibaryon. This is constructed in Sec. II C.

A. The eLSM Lagrangian for nucleons

In the mirror assignment and in the two-flavor case, the eLSM Lagrangian in the nucleon sector has the form [23]

$$\begin{aligned}\mathcal{L}_{eLSM} = {} & \bar{\Psi}_{1L} i\gamma_\mu D^\mu_{1L} \Psi_{1L} + \bar{\Psi}_{1R} i\gamma_\mu D^\mu_{1R} \Psi_{1R} \\ & + \bar{\Psi}_{2L} i\gamma_\mu D^\mu_{2R} \Psi_{2L} + \bar{\Psi}_{2R} i\gamma_\mu D^\mu_{2L} \Psi_{2R} \\ & - \hat{g}_1(\bar{\Psi}_{1L}\Phi\Psi_{1R} + \bar{\Psi}_{1R}\Phi^\dagger\Psi_{1L}) \\ & - \hat{g}_2(\bar{\Psi}_{2L}\Phi^\dagger\Psi_{2R} + \bar{\Psi}_{2R}\Phi\Psi_{2L}) \\ & - a\chi(\bar{\Psi}_{1L}\Psi_{2R} - \bar{\Psi}_{1R}\Psi_{2L} - \bar{\Psi}_{2L}\Psi_{1R} + \bar{\Psi}_{2R}\Psi_{1L}),\end{aligned} \tag{1}$$

where

(i) The first line of Eq. (1) describes the interaction of the nucleons with (axial-)vector mesons via the derivatives $D_{1(2)L(R)}$, which are defined as

$$D^\mu_{1R} = \partial^\mu - ic_1 R^\mu, \quad D^\mu_{1L} = \partial^\mu - ic_1 L^\mu, \tag{2}$$

$$D^\mu_{2R} = \partial^\mu - ic_2 R^\mu, \quad D^\mu_{2L} = \partial^\mu - ic_2 L^\mu. \tag{3}$$

The left-handed and right-handed fields L^μ and R^μ contain the vector mesons ω^μ_N and $\vec{\rho}^\mu$ and the axial-vector mesons $f^\mu_{1,N}$ and $\vec{a}^\mu_1$:

$$L^\mu = (\omega^\mu_N + f^\mu_{1,N})t^0 + (\vec{\rho}^\mu + \vec{a}^\mu_1)\cdot\vec{t}, \tag{4}$$

$$R^\mu = (\omega^\mu_N - f^\mu_{1,N})t^0 + (\vec{\rho}^\mu - \vec{a}^\mu_1)\cdot\vec{t}, \tag{5}$$

where t^0 and $\vec{t}$ represent the isospin matrices [$t^0 = 1_2/2$ is half the (2×2) unit matrix and $\vec{t} = \vec{\sigma}/2$, σ_i being the ith Pauli matrix]. The correspondence of the fields to quark-antiquark mesons listed in the PDG [38] is reported in Table I. Vector mesons are an important ingredient for a good description of low-energy nucleon vacuum phenomenology; see, e.g., Refs. [23,39].

(ii) The second line of Eq. (1) describes the interaction of the nucleons with the (pseudo)scalar mesons, parametrized in terms of the matrix

$$\Phi = (\sigma_N + i\eta_N)t^0 + (\vec{a}_0 + i\vec{\pi})\cdot\vec{t}; \tag{6}$$

see again Table I for the field-resonance correspondence. [Note that the field η_N has quark content $(u\bar{u} + d\bar{d})/\sqrt{2}$ and can be expressed as a combination of the physical fields η and η' as $\eta_N = \cos\varphi_P\eta - \sin\varphi_P\eta'$ where the mixing angle is $\varphi_P \approx -44^\circ$ [21]; in the other sectors we neglect the small strange-nonstrange mixing.] The interaction terms in the second line provide a contribution to the nucleon masses via the condensation of σ ($\sigma \to \sigma + \phi$, where ϕ is the chiral condensate). In the original linear sigma model, this was the only contribution to the nucleon mass in the chiral limit. Note that the resonances $a_0(980)$, $f_0(980)$, and $K_0^*(800)$ are not included in the model since they turn out to be predominantly four-quark objects; see, e.g., Refs. [30,40–42] and references therein. Namely, these resonances form, together with the resonance $f_0(500)$, a nonet of nonconventional mesons. As we discuss below, in the $N_f = 2$ framework adopted in this work, only $f_0(500)$ will be considered [since it has no (open or hidden) strangeness content in its wave function].

(iii) The third and last line of Eq. (1) describes the interaction of the nucleon fields Ψ_1 and Ψ_2 with the scalar nonconventional meson χ. The latter gives a contribution to the nucleon masses due to the condensation of χ ($\chi \to \chi + \chi_0$). The mass parameter

$$m_0 = a\chi_0 \tag{7}$$

was discussed in the pioneering work of Ref. [26] and further investigated in Refs. [23–25,27,28]. In Ref. [33] it was suggested that the mass term m_0 arises from the condensation of the scalar isoscalar field χ.

[1]Although SAID provides consistent total and differential np scattering cross sections summed over both isospin channels, the individual $I = 0$ and $I = 1$ differential np scattering cross sections seem to be wrong by a factor of 2. In our analysis, we have taken this factor into account, i.e., we divided SAID data by a factor of 2.

TABLE I. Correspondence of the fields to mesons listed in Ref. [38].

Field	PDG	Quark content	I	J^{PC}	Mass (GeV)
π^+,π^-,π^0	π	$u\bar{d},d\bar{u},\frac{u\bar{u}-d\bar{d}}{\sqrt{2}}$	1	0^{-+}	0.13957
η	$\eta(547)$	$\frac{u\bar{u}+d\bar{d}}{\sqrt{2}}\cos\varphi_P - s\bar{s}\sin\varphi_P$	0	0^{-+}	0.54786
η'	$\eta'(958)$	$\frac{u\bar{u}+d\bar{d}}{\sqrt{2}}\sin\varphi_P + s\bar{s}\cos\varphi_P$	0	0^{-+}	0.95778
a_0^+,a_0^-,a_0^0	$a_0(1450)$	$u\bar{d},d\bar{u},\frac{u\bar{u}-d\bar{d}}{\sqrt{2}}$	1	0^{++}	1.474
σ_N	$f_0(1370)$	$\frac{u\bar{u}+d\bar{d}}{\sqrt{2}}$	0	0^{++}	1.350
ρ^+,ρ^-,ρ^0	$\rho(770)$	$u\bar{d},d\bar{u},\frac{u\bar{u}-d\bar{d}}{\sqrt{2}}$	1	1^{--}	0.77526
ω_N	$\omega(782)$	$\frac{u\bar{u}+d\bar{d}}{\sqrt{2}}$	0	1^{--}	0.78265
a_1^+,a_1^-,a_1^0	$a_1(1230)$	$u\bar{d},d\bar{u},\frac{u\bar{u}-d\bar{d}}{\sqrt{2}}$	1	1^{++}	1.230
$f_{1,N}$	$f_1(1285)$	$\frac{u\bar{u}+d\bar{d}}{\sqrt{2}}$	0	1^{++}	1.2819
χ	$f_0(500)$	$\pi\pi$ or $[u,d][\bar{u},\bar{d}]$	0	0^{++}	0.475

The latter corresponds to the resonance $f_0(500)$ in the context of nuclear physics [33,34].

Finally, the nucleon fields Ψ_1 and Ψ_2 are related to the physical states of the nucleon N and its chiral partner N^* as

$$\Psi_1 = \frac{1}{\sqrt{2\cosh\delta}}(Ne^{\delta/2} + \gamma_5 N^* e^{-\delta/2}), \tag{8}$$

$$\Psi_2 = \frac{1}{\sqrt{2\cosh\delta}}(\gamma_5 Ne^{-\delta/2} - N^* e^{\delta/2}), \tag{9}$$

where

$$\cosh\delta = \frac{m_N + m_{N^*}}{2m_0}. \tag{10}$$

The field N corresponds to the nucleon $N(939)$ while N^* to its chiral partner, which could be $N(1535)$ or $N(1650)$. For the purposes of the present work, the assignment of N^* is not crucial. For the sake of definiteness, we will use the results of Ref. [24], in which $N(1650)$ is regarded as the chiral partner. On the other hand, in an enlarged mixing scenario [25], $N(1535)$ is favored as the chiral partner of the nucleon. However, using this alternative scenario does not lead to noticeable quantitative changes of our results.

The masses of the nucleon N and its chiral partner N^* are given by

$$m_{N,N^*} = \sqrt{m_0^2 + \frac{(\hat{g}_1+\hat{g}_2)^2}{16}\phi^2} \pm \frac{1}{4}(\hat{g}_1 - \hat{g}_2)\phi. \tag{11}$$

In the limit $m_0 \to 0$, one obtains the result $m_N = \hat{g}_1\phi/2$; i.e., the nucleon mass is solely generated by the chiral condensate (as in the original linear sigma model [16,17]).

Using the Lagrangian of Eq. (1), we also obtain expressions for the axial coupling constants g_A^N and $g_A^{N^*}$ of the nucleon and its chiral partner N^*, respectively:

$$g_A^N = \frac{1}{2\cosh\delta}\left(g_A^{(1)}e^{\delta} + g_A^{(2)}e^{-\delta}\right),$$
$$g_A^{N^*} = \frac{1}{2\cosh\delta}\left(g_A^{(1)}e^{-\delta} + g_A^{(2)}e^{\delta}\right), \tag{12}$$

where

$$g_A^{(1)} = 1 - \frac{c_1}{g_1}\left(1 - \frac{1}{Z^2}\right), \quad g_A^{(2)} = -1 + \frac{c_2}{g_1}\left(1 - \frac{1}{Z^2}\right). \tag{13}$$

We recall that $Z = (1 - g_1 w\phi)^{-1/2} = 1.67 > 1$, where $g_1 = 5.84$ describes the coupling constant of (pseudo)scalar and (axial-)vector mesons, and $w = g_1\phi/m_{a_1}^2$. This parameter arises from the mixing of pseudoscalar and axial-vector mesons; see Refs. [19,21]. As a consequence, the condensate reads $\phi = Zf_\pi$, where $f_\pi = 0.0924$ GeV is the pion decay constant. The importance of vector mesons is evident, since only for nonzero c_1 and c_2 (and for $Z > 1$), it is possible to get an agreement of the axial coupling constants with experimental data and lattice-QCD calculations [43].

In total, the nucleon part of the model has five independent parameters $(a,\hat{g}_1,\hat{g}_2,c_1,c_2)$, which are determined by using the PDG values $m_N = 0.939$ GeV, $m_{N^*} = 1.650$ GeV, $\Gamma_{N^*\to NP} = 0.128$ GeV, the axial coupling constant $g_A^N = 1.267$, as well as lattice-QCD calculations of the axial coupling constant $g_A^{N^*} = 0.55$ [43], for details and determination of the errors; see Ref. [23]. Explicitly,

$$c_1 = -3.34, \quad c_2 = 14.74, \quad \hat{g}_1 = 9.47\,, \quad \hat{g}_2 = 18.69,$$
$$m_0 = 0.704 \text{ GeV}. \tag{14}$$

Finally, as described in Ref. [33], the condensate χ_0 takes the form $\chi_0 = g_{\chi\pi\pi}\phi^2/m_\chi^2$, where $g_{\chi\pi\pi}$ is the $\chi\pi\pi$ coupling constant [40,44]. Its numerical value was determined to be 0.45 GeV [33] by requiring a correct description of the nuclear matter ground state. Since we assign $\chi \equiv f_0(500)$, we use $m_\chi = (0.475 \pm 0.25)$ GeV [38]. As a consequence of $\chi_0 = g_{\chi\pi\pi}\phi^2/m_\chi^2$, the constant a in Eq. (1) reads

$$a = \frac{m_0}{\chi_0} = \frac{m_0 m_\chi^2}{g_{\chi\pi\pi}(Zf_\pi)^2}, \tag{15}$$

which equals 14.8 for $m_\chi = 0.475$ GeV.

The value of a as given by Eq. (15) is the maximum value for the coupling of χ to nucleons. If other scalar condensates (e.g., a glueball condensate) contribute to the mass parameter m_0, Eq. (7), the value of a would be reduced. Hence, for the results presented in Sec. III we will choose also lower values for a than given by Eq. (15), if necessary to achieve good agreement with SAID results.

B. Lagrangian for nucleon-nucleon elastic scattering

Only some of the terms contained in Eq. (1) contribute to elastic nucleon-nucleon scattering (for instance, the nucleon resonance N^* does not contribute). We thus split the full Lagrangian $\mathcal{L}_{eLSM} = \mathcal{L}_{NN} + \mathcal{L}_{rest}$, where the relevant terms for our calculations are contained in $\mathcal{L}_{NN}$. Its explicit form in terms of physical fields reads

$$\begin{aligned}\mathcal{L}_{NN} = \frac{1}{2\cosh\delta}\big(&e^{\delta} c_1 \overline{N}\big\{\omega_N^\mu t^0 + \vec{\rho}^\mu\cdot\vec{t} + \big[f_{1,N}^\mu t^0 + \vec{a}_1^\mu\cdot\vec{t} + wZ(\partial_\mu\eta_N t^0 + \partial_\mu\vec{\pi}\cdot\vec{t})\big]\gamma_5\big\}\gamma_\mu N\\ &+ e^{-\delta} c_2 \overline{N}\big\{\omega_N^\mu t^0 + \vec{\rho}^\mu\cdot\vec{t} - \big[f_{1,N}^\mu t^0 + \vec{a}_1^\mu\cdot\vec{t} + wZ(\partial_\mu\eta_N t^0 + \partial_\mu\vec{\pi}\cdot\vec{t})\big]\gamma_5\big\}\gamma_\mu N\\ &- e^{\delta}\hat{g}_1\overline{N}\{[(\sigma_N+\varphi)t^0 + \vec{a}_0\cdot\vec{t}\,] + iZ(\eta_N t^0 + \vec{\pi}\cdot\vec{t})\gamma_5\}N\\ &+ e^{-\delta}\hat{g}_2\overline{N}\{[(\sigma_N+\varphi)t^0 + \vec{a}_0\cdot\vec{t}\,] - iZ(\eta_N t^0 + \vec{\pi}\cdot\vec{t})\gamma_5\}N - 2a\overline{N}(\chi+\chi_0)N\big).\end{aligned} \tag{16}$$

The resulting t- and u-channel Feynman diagrams for nucleon-nucleon interactions via meson exchange are shown in Fig. 1. We use the following propagators for the exchanged mesons:

$$G_S = \frac{i}{q^2 - m_i^2}, \quad G_{V,\alpha\beta} = -i\left(g_{\alpha\beta} - \frac{q_\alpha q_\beta}{m_i^2}\right)\frac{1}{q^2 - m_i^2} \tag{17}$$

for spinless and spin-1 particles, respectively; m_i denotes the on-shell mass of the exchanged meson.

As a last point, we describe the introduction of form factors. The model described in Eq. (1) is not a fundamental model which describes the interactions of point-like particles, but an effective model whose degrees of freedom are hadrons (nucleons and mesons) which have a finite extension ($\sim$0.5 fm). Therefore, the tree-level diagrams derived from the Lagrangian (1) are valid when the momentum exchanged at a certain vertex is smaller than $\sim 2\ \mathrm{fm}^{-1} \simeq 0.4$ GeV. Therefore, as various works have shown—see, e.g., Refs. [45–48] and also Ref. [38] (see the section "Quark Model in Standard Model and Related Topics")—and as we shall also see later on, it is important to introduce a form factor which reduces the interaction strength when the momenta of the hadrons are large. In this work we will use the following form factor attached to each nucleon-nucleon-meson vertex:

$$F(q^2) = \exp\left(-\frac{|q^2 - m_i^2|}{\Lambda_{\mathrm{cut}}^2}\right), \tag{18}$$

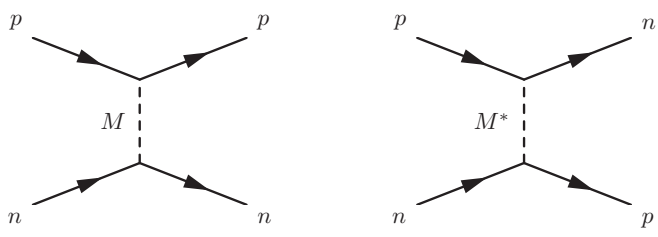

FIG. 1. Feynman diagrams for np scattering in the eLSM. Left: neutral meson exchange, $M \equiv \chi,\sigma,a_0^0,\pi^0,\eta,\omega,\rho^0,f_1,a_1^0$. Right: charged meson exchange, $M^* \equiv a_0^\pm,\pi^\pm,\rho^\pm,a_1^\pm$.

where q^2 is the square of the four-momentum transfer involved in the process (q^μ is the four-momentum of the exchanged meson, and m_i its mass, $i = \pi,\rho,\ldots$). The parameter Λ_{cut} is a hadronic energy scale, which is $\sim$1 GeV.

An alternative approach to form factors is the implementation of unitarization approaches (such as the so-called K-matrix unitarization) which also cause a decrease of cross section at high energies. However, their use would imply the need for a partial-wave analysis which goes beyond the scope of the present paper. We leave this study as well as the analysis of neutron-proton scattering in all partial waves (see, e.g., Ref. [12]) for the future.

C. Interaction Lagrangian for the $^1S_0$ dibaryon

The interaction of nucleons via meson exchange is not capable of describing the large cross section close to threshold. Namely, the interaction strength is three orders of magnitude larger than what can be achieved through meson exchange: a neutron-proton resonance is responsible for the enhanced cross section.

In order to describe this resonance within our framework, we introduce a new field, denoted as Φ_R, which has quantum numbers $I = 1$, $J^P = 0^+$ (also known as $^1S_0$) and contributes to $I = 1$ np scattering close to threshold. The wave function of the $I_z = 0$ component (of relevance for the following) is given by

$$|\Phi_R\rangle = |\text{space: ground state}\rangle|\uparrow\downarrow - \downarrow\uparrow\rangle|np + pn\rangle. \tag{19}$$

Being part of an isospin multiplet, there are two analogous states, $|pp\rangle$ with $I_z = 1$, and $|nn\rangle$ with $I_z = -1$; see the corresponding discussion in Sec. IV.

The Lagrangian coupling Φ_R to nucleons is given by

$$\mathcal{L}_R = iG_R(N^T C\gamma^5\Phi_R t^1 N + \bar{N}\gamma^5\Phi_R^* t^1 C\bar{N}^T), \tag{20}$$

where C denotes the charge-conjugation matrix. The first term on the right-hand side of Eq. (20) describes the two incoming nucleons creating the dibaryon, while the other term describes the decay of the dibaryon into two outgoing nucleons. A similar Lagrangian for the deuteron was studied in Ref. [46]. The

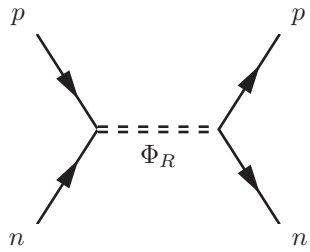

FIG. 2. Feynman diagram for $I = 1$ np scattering via the charged $^1S_0$ resonance.

corresponding Feynman diagram for np scattering is shown in Fig. 2.

Using Eq. (20) we calculate the width $\Gamma(p)$ of the $^1S_0$ state as

$$\Gamma(p) = \frac{G_R^2 p}{4\pi}, \tag{21}$$

where p denotes the modulus of the three-momentum of an outgoing nucleon. The propagator of the $^1S_0$ state is given by

$$\Delta_R(s) = \frac{i}{s - m_R^2 + i\sqrt{s}\,\Gamma(p)}, \tag{22}$$

where m_R denotes the "mass" of the dibaryon resonance. We recall that p is a function of the kinematic variable s,

$$p = p(s) = \sqrt{\frac{s^2 + \left(m_p^2 - m_n^2\right)^2 - 2s\left(m_p^2 + m_n^2\right)}{4s}}, \tag{23}$$

where m_p and m_n are the proton and the neutron masses, respectively. For a good description of SAID results it is essential to consider the decay width as a function of p, i.e., $\Gamma(p)$. Setting the decay width to a constant, $\Gamma_R \equiv \Gamma(p_R)$, where $p_R \equiv p(m_R^2)$, (i.e., the Breit-Wigner limit) is definitely not a good approximation in the present context. Hence, the quantity m_R should not be regarded as a conventional resonance mass, but as a parameter corresponding to the root of the real part of the denominator of the propagator; see also the discussion in Sec. III A.

At the end of this section, two comments are in order:

(i) The propagator (22) emerges upon a resummation of proton-neutron loops. In this respect, it corresponds to a (partial) unitarization in the s channel for this particular process. Note, for simplicity the real part of the propagator's denominator has not been modified (see Sec. III A).

(ii) As discussed in Refs. [1,10,12], it is not necessary to introduce an additional field Φ_R to describe data. One would obtain an equally good description by starting with a quartic interaction term proportional to $(N^T C\gamma^5 t^1 N)^2$ and by doing a resummation of the proton-neutron loop emerging from it. This S-wave resummation generates an expression which resembles that of a propagator of a scalar particle. Then, in the framework of an correct description of data, the inclusion of an explicit dimeron field Φ_R is possible but not necessary. Yet, the point that we would like to address is if a pole in the complex plane on the second Riemann sheet exists. Namely, this is the condition that should be met for a state to exist. In fact, the position of the pole is independent on the particular process and (in principle) is also independent on the particular Lagrangian employed, as long as data are correctly described. Indeed, we show in the next section that we do find a pole in the complex plane.

III. RESULTS

We now turn to the results. We present them successively including more ingredients: (i) we consider only the scalar dibaryon [Eq. (20)]; (ii) we consider a reduced model with the dibaryon and the scalar meson $\chi \equiv f_0(500)$ [Eq. (20) and the last line of Eq. (16)]; (iii) we include all other mesons without form factor [Eqs. (16) and (20) with $\Lambda_{\rm cut} \to \infty$]; (iv) we include also a form factor [Eqs. (16) and (20) with finite $\Lambda_{\rm cut}$].

In all cases, the cross section for np scattering in the $I = 1$ channel was calculated by splitting the scattering amplitude $\mathcal{M}$ into two parts, $\mathcal{M}_{I=0}$ and $\mathcal{M}_{I=1}$, according to the formalism presented in Ref. [49]. The masses of the neutron and proton were set equal to 938.919 MeV (the average of both masses), except for the study of the pole and spectral function of the $^1S_0$ dibaryon resonance, which was done using the masses reported in Ref. [38]. The results were cross-checked by calculating the cross section for pp scattering neglecting Coulomb interaction using the programs FEYNRULES 2.0 [50] and MADGRAPH 2.3.0 [51]. Results of both calculations were identical within numerical precision.

A. Scalar dibaryon only

We first consider the case where only the Lagrangian (20) is considered. The interaction is mediated by the dibaryon resonance Φ_R. Figure 3(a) shows the total cross section for different values of $D_R = m_R - m_p - m_n$, where m_R is the mass parameter entering Eq. (22). As one observes, the total cross section is very large at threshold and drops rapidly with increasing momentum. The best agreement with SAID results is obtained for the dibaryon coupling strength $G_R = 2.13$ and for $D_R = 0.0015$ GeV. Namely, we obtain a good description of the SAID results over three orders of magnitudes up to a c.m. momentum of about 0.2 GeV. Clearly, the calculation using only the $^1S_0$ resonance cannot describe the SAID results at higher momenta. For momenta above 0.2 GeV, the interaction via meson exchange (as, for instance, described via the eLSM Lagrangian) dominates.

As expected, there is no angular dependence (at any p) of the theoretically calculated differential cross section when only the dibaryon is included; see Fig. 3(b). On the contrary, SAID results show an enhancement at forward and backward angles. This enhancement increases with momentum and, as we shall see, can be explained considering meson exchange [in particular $f_0(500)$].

In conclusion, we find that there is an isotriplet dibaryon resonance with nominal mass $m_R = m_p + m_n + 0.0015$ GeV. The corresponding on-shell decay width is $\Gamma_R = 0.0135$ GeV,

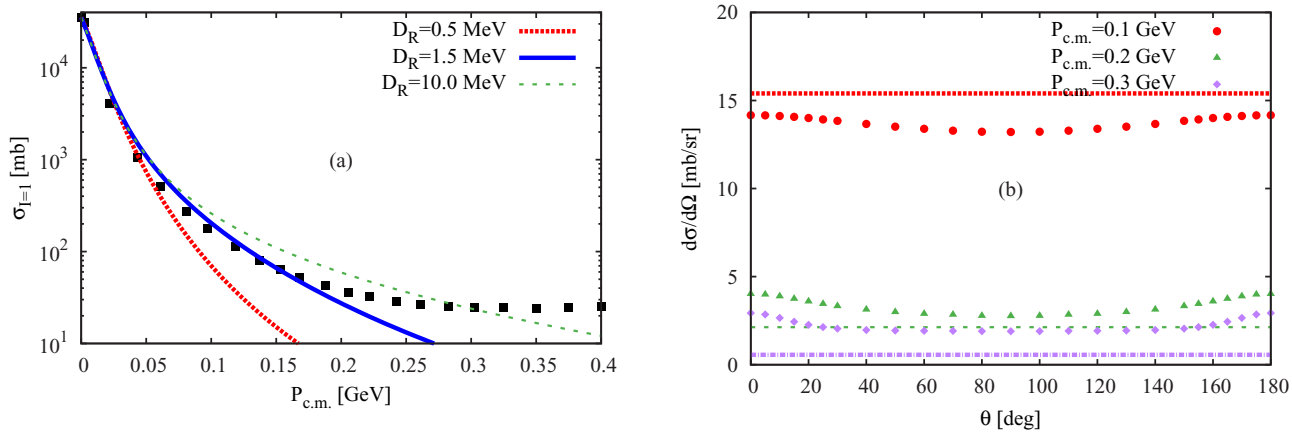

FIG. 3. Total (a) and differential (b) cross section for $I = 1$ np scattering via the ${}^1S_0$ resonance only. In (a), the total cross section is shown for different values of $D_R = 0.0005$ GeV (red dotted curve), 0.0015 GeV (blue solid curve), and 0.01 GeV (green dashed curve). The corresponding values for G_R (chosen to fit the total cross section at threshold) are 1.23, 2.13, and 5.5, respectively. In (b), the differential cross section is shown for $D_R = 0.0015$ GeV and $G_R = 2.13$ for nucleon c.m. momenta 0.1 GeV (red dotted curve), 0.2 GeV (green dashed curve), and 0.3 GeV (magenta dash-dotted curve), respectively. Data points are taken from the SAID program [36].

which is much larger than D_R. Whenever the tree-level decay width is comparable to or larger than the distance of the mass from the threshold, we are not dealing with a standard resonance; see, e.g., Ref. [52] and references therein. Here, the situation is even more extreme, since $\Gamma_R \gg D_R$. This is also why many authors were extremely careful in discussing this putative state as a standard resonance.

In the literature, it is common to investigate the existence and position of pole(s) in the complex $\sqrt{s}$ plane, especially in presence of wide resonances [as, for instance, in the renowned case of the resonance $f_0(500)$; see Ref. [32] and references therein]. To this end, we investigate the presence of a pole by using the formalism discussed in Ref. [41]: we introduce a form factor in the decay width, $\Gamma(p) \to \Gamma_{\Lambda_R}(p) = \Gamma(p)e^{-2p^2/\Lambda_R^2}$. Then, according to the optical theorem, the one-loop self-energy $\Sigma(s)$ (which consists of a neutron-proton loop) fulfills $\mathrm{Im}\,\Sigma(s) = \sqrt{s}\Gamma_{\Lambda_R}(p)$. The real part is determined by using the dispersion integral

$$\mathrm{Re}\,\Sigma(s) = -\frac{1}{\pi}\,\mathrm{P.V.}\int_{m_p+m_n}^{\infty} ds'\,\frac{\mathrm{Im}\,\Sigma(s')}{s-s'}, \qquad (24)$$

where P.V. stands for principal value. The dressed propagator of the dibaryon reads

$$\Delta_R^{\mathrm{dressed}}(s) = \frac{1}{s - m_R^2 + \mathrm{Re}\,\Sigma(s) - \mathrm{Re}\,\Sigma\left(m_R^2\right) + i\,\mathrm{Im}\,\Sigma(s)}, \qquad (25)$$

while its spectral function is given by

$$d_R(\sqrt{s}) = \frac{2\sqrt{s}}{\pi}\,\mathrm{Im}\,\Delta_R^{\mathrm{dressed}}(s). \qquad (26)$$

The latter is plotted in Fig. 4 using $\Lambda_R = 0.5$ GeV (close to the values obtained in Refs. [41,42]). One notices a peak very close to threshold (only 0.000 0174 GeV away from it) and then a rapid descent. Note that the peak does not correspond to the nominal mass m_R. Since Λ_R is a free parameter, we also show the spectral function for $\Lambda_R = 0.3$ GeV. The quantitative difference to the previous case is small, the qualitative features remain the same.

Note that, in principle, one should have used from the very beginning the propagator (25) in the calculation of the cross section. Such a calculation would require to determine the parameter G_R in a set of complicated coupled equations. In view of the uncertainty on Λ_R, such a procedure, while formally correct, goes beyond the scope of the present work. However, we have *a posteriori* verified that the full propagators (22) and (25) deliver similar results for the cross section.

Finally, we turn to the position of the pole of the dimeron. For $\Lambda_R = 0.5$ GeV we find a pole for

$$\sqrt{s_{\mathrm{pole}}} = m_p + m_n + 0.014\ \mathrm{GeV} - i\,0.0774\ \mathrm{GeV}\,. \qquad (27)$$

We observe that the decay width associated with the imaginary part of the pole is much larger than the tree-level decay width: $\Gamma_{\mathrm{pole}} = 0.1548$ GeV. In addition, the pole mass, being

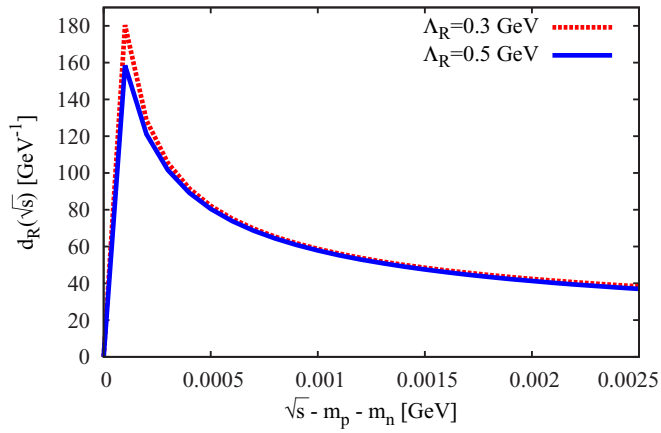

FIG. 4. Spectral function of the scalar dibaryon as function of $\sqrt{s} - m_p - m_n$ for $\Lambda_R = 0.5$ GeV and $\Lambda_R = 0.3$ GeV. We verified that the spectral functions are correctly normalized to unity.

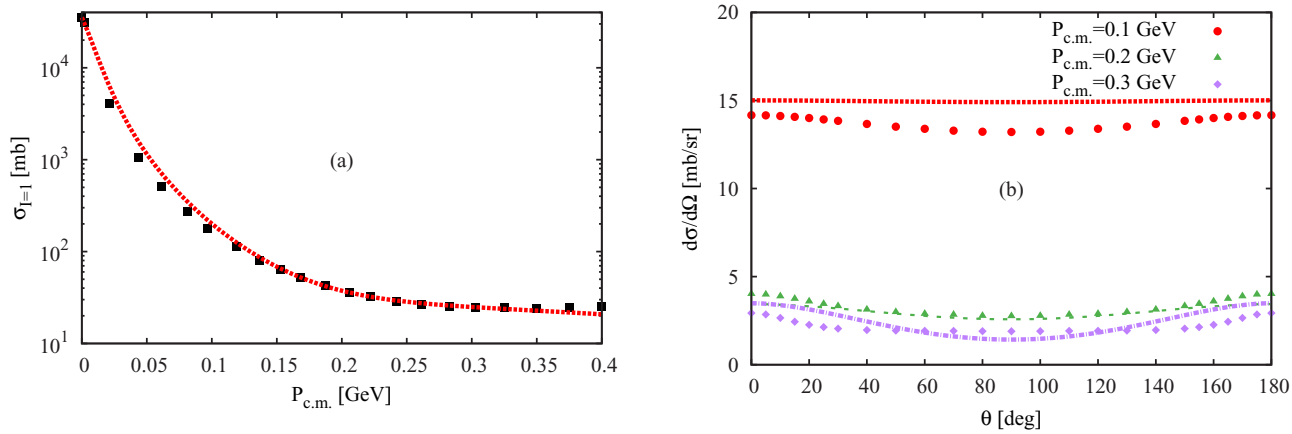

FIG. 5. Total (a) and differential (b) cross section for $I = 1$ np scattering. The theoretical curve in (a) is calculated for scattering including χ exchange in addition to the contribution of the $^1S_0$ resonance with $D_R = 0.0018$ GeV and $G_R = 2.27$. The mass of the χ meson is set to 0.525 GeV and its coupling $a = 8.95$. In (b), the differential cross section is shown for nucleon c.m. momenta 0.1 GeV (red dotted curve), 0.2 GeV (green dashed curve), and 0.3 GeV (magenta dash-dotted curve), respectively. Data points are taken from the SAID program [36].

0.014 GeV above the threshold, is larger. For this very peculiar resonance there is no correspondence between nominal mass, peak of the spectral function, and pole mass.

For $\Lambda_R = 0.3$ GeV, the pole is located at

$$\sqrt{s_{\rm pole}} = m_p + m_n + 0.0273\ \text{GeV} - i\,0.0309\ \text{GeV}, \quad (28)$$

which has a larger mass but a smaller width. While the spectral function changes only slightly by changing Λ_R, the position of the pole changes sizably. The precise determination of the pole is not possible at present, since the value of Λ_R (as well as the precise form of the form factor) is unknown. Nevertheless, the existence of a pole in the complex $\sqrt{s}$ plane is a definite result of our analysis.

B. Dibaryon and $f_0(500)$

In the next step, we add the contribution from $\chi \equiv f_0(500)$ [last line of Eq. (16)] to that of the dibaryon state of Eq. (20). Using $m_\chi = 0.525$ GeV and $a = 8.95$, it is indeed possible to obtain a remarkably good agreement with SAID results up to a momentum p of about 0.4 GeV; see Fig. 5. This shows the importance of the lightest scalar state $f_0(500)$. We recall that this meson is not (predominantly) a quark-antiquark state (the chiral partner of the pion is identified with the heavier state $f_0(1370)$ [21]). Also the description of the differential cross section is improved, since now the qualitative form is correctly described (for $p = 0.2$ GeV the agreement is also quantitatively quite good).

It is interesting to notice that good agreement with SAID results is reached for a mass of $f_0(500)$ of about 0.5–0.55 GeV, which is in good agreement with the PDG value. Increasing or decreasing the value of the mass by about 0.1 GeV or more considerably worsens the description of the experimental results.

C. Full model without form factor

We now turn to the case in which the sum of the two Lagrangians (16) and (20) is considered, i.e., when all other mesons are also present. First, we do not include any form factor in the calculation (i.e., $\Lambda_{\rm cut} \to \infty$). The mass of $f_0(500)$ is chosen to be $m_\chi = 0.475$ GeV and $a = 8.95$.

The results are shown in Fig. 6. In part (a), one observes that the theoretically calculated total cross section significantly overestimates the SAID results for large momenta. The reason for this is the contribution from the pseudoscalar mesons (green dashed curve). In addition, the theoretically calculated differential cross sections, part (b), show the wrong behavior as a function of scattering angle: they are enhanced at 90^0, while the SAID results are suppressed.

Apparently, adding the contributions from exchange of quark-antiquark mesons worsens the agreement with SAID results as compared to the previous case. One possibility to ameliorate the situation could be to modify the parameters of the Lagrangian (1). Quite curiously, for $c_1 = 1.5$ the contribution of the pions turns out to be suppressed due to destructive interference. However, by doing so, one would inevitably induce a disagreement with other quantities, such as the nucleon masses and the axial coupling constants. Another possibility, explored in the following subsection, is to use a finite cutoff, which effectively takes into account that hadrons are extended objects, and which suppresses the contribution from pseudoscalar mesons to an extent that the good description obtained with the $^1S_0$ resonance and $f_0(500)$ exchange alone is reobtained.

D. Full model with form factors

As a last step we consider both Lagrangians (16) and (20) as well as the form factor introduced in Eq. (18). As Fig. 7 shows, a cutoff $\Lambda_{\rm cut} = 0.778$ GeV suppresses the contributions of the quark-antiquark mesons (and in particular pseudoscalar mesons) at large momenta. The SAID results can be again well described.

The differential cross sections point also to an interesting fact: if the contribution from $f_0(500)$ is turned off, the angular distribution is again enhanced at 90^0, in contradiction with SAID results which are suppressed at this angle. When $f_0(500)$

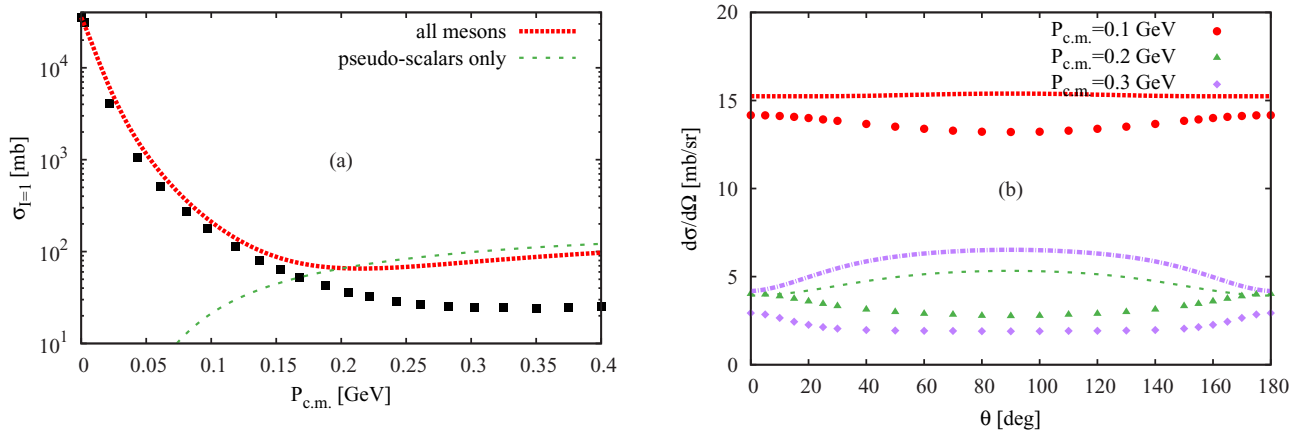

FIG. 6. Total (a) and differential (b) cross section for $I = 1$ np scattering. The red dotted curve in (a) is for scattering via exchange of the nine mesons included in Eq. (16) ($m_\chi = 0.475$ GeV and $a = 8.95$) in addition to the $^1S_0$ resonance with $D_R = 0.0018$ GeV and $G_R = 2.26$. The green dashed curve shows the cross section calculated using only π and η exchange. In (b), the differential cross section is shown for nucleon c.m. momenta 0.1 GeV (red dotted curve), 0.2 GeV (green dashed curve), and 0.3 GeV (magenta dash-dotted curve) upon exchange of the nine mesons. Data points are taken from the SAID program [36].

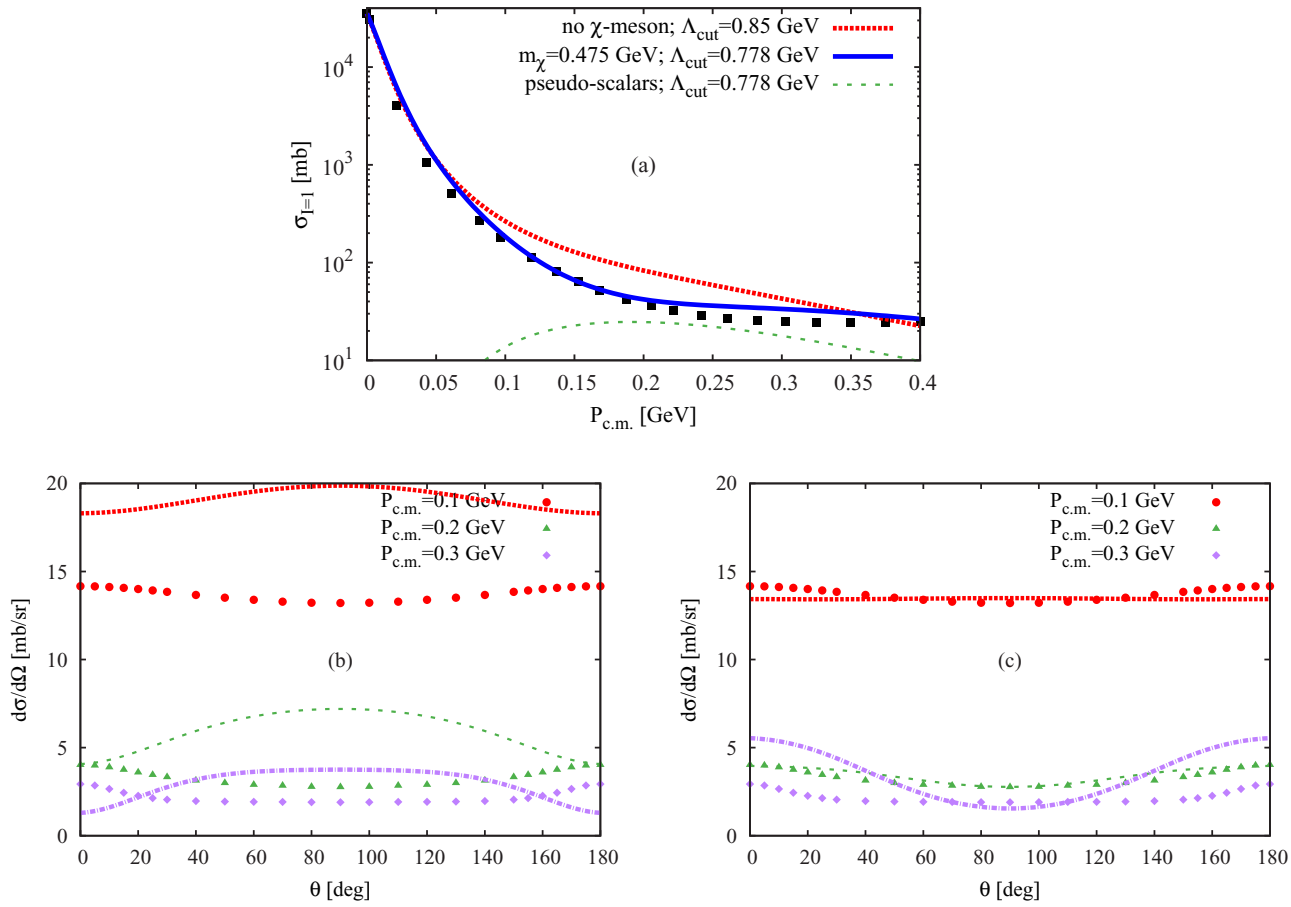

FIG. 7. Total (a) and differential cross sections (b,c) for $I = 1$ np scattering. The red dotted and blue solid curves in Fig. a are calculated for $\sigma,a_0,\pi,\eta,\omega,\rho,f_1,a_1$ exchange as well as including the $^1S_0$ resonance with $D_R = 0.0016$ GeV. The red dotted curve shows the case without the χ meson ($\Lambda_{\rm cut} = 0.85$ GeV), while the blue solid curve shows the case where a χ meson with mass $m_\chi = 0.475$ GeV and coupling $a = 12.41$ is included ($\Lambda_{\rm cut} = 0.778$ GeV). The green dashed curve shows the cross section calculated using only π and η exchange. Panel (a) [(c)] shows the differential cross section without [with] χ meson exchange and $\Lambda_{\rm cut} = 0.85$ GeV [0.778 GeV] upon inclusion of the eight other mesons, for nucleon c.m. momenta 0.1 GeV (red dotted curve), 0.2 GeV (green dashed curve), and 0.3 GeV (magenta dash-dotted curve), respectively. Data points are taken from the SAID program [36].

is taken into account, the correct shape of the differential cross section is obtained. Apparently, suppressing the contribution of quark-antiquark mesons by a form factor is not sufficient to produce the correct angular dependence of the differential cross section, one needs to include the $f_0(500)$ in order to repair this shortcoming. This confirms once more the important role of this meson for a good description of nucleon-nucleon scattering.

IV. CONCLUSIONS

In this work, we have studied neutron-proton scattering in the $I = 1$ channel in the framework of a chiral model which contains quark-antiquark (pseudo)scalar and (axial-)vector mesons as well as a scalar isoscalar state corresponding to the resonance $f_0(500)$ (see Fig. 1 for the corresponding diagrams). The $f_0(500)$ state is coupled to nucleons in a chirally invariant way using the mirror assignment for the chiral partner of the nucleon.

The exchange of mesons (Fig. 1) alone is not sufficient to describe the very large total cross section close to threshold. For this reason, we have coupled the nucleons to a resonance with baryon number $B = 2$, isospin $I = 1$, total spin zero, and positive parity, $J^P = 0^+$. Then, for a suitably chosen coupling to the nucleons, s-channel scattering through this resonance is able to reproduce the magnitude of the total cross section close to threshold; see Fig. 2.

The results have been presented by including the ingredients step by step. The total cross section close to threshold can be well described with the help of the dibaryon alone (Fig. 3). A more detailed study of this resonance shows that it is not of a standard Breit-Wigner type, because the width is larger than the distance of its mass to the neutron-proton threshold. Its spectral function (Fig. 4) shows a peak very close to threshold. In the complex plane, we find a pole. For a cutoff of 0.5 GeV the pole lies at $m_p + m_n + 0.014\text{GeV} - i\,0.0774\text{GeV}$, confirming that the resonance is very broad. However, the pole is not precisely determined because a slight modification of the parameters changes its position quite substantially. Nevertheless, the important point is that a pole is always present, which shows that a dibaryon resonance exists. Interestingly, a similar conclusion concerning a metastable neutron-proton state was also obtained in Ref. [53] and recent experimental activity is described in Ref. [54].

As a consequence of our results, we also predict the existence of a neutron-neutron resonance very close to threshold: this state is the $I_z = -1$ member of the $I = 1$ multiplet of scalar dibaryons. The neutron-neutron resonance is not affected by Coulomb repulsion, thus the characteristics of the corresponding resonance are expected to be similar to the proton-neutron dibaryon studied in this work. Indeed, in Ref. [55] a scalar neutron-neutron resonance has been observed experimentally. The corresponding decay width of about 0.01 GeV is actually in good agreement with our results (for the width of the np state, which should be very similar to the one of the nn state). The subsequent theoretical study of Ref. [56] by means of an effective Lagrangian confirmed that such a dineutron state cannot be excluded. Quite interestingly, the existence of scalar isotriplet dibaryon may also be relevant in the context of nuclear astrophysics [57]. Also, the recent discovery of a four-neutron quasibound state [58] shows that the formation of metastable states made solely of neutrons is possible.

The last member of the isotriplet dibaryon multiplet has $I_z = 1$ and consists of two protons. In this channel predictions are more difficult in view of the Coulomb repulsion that breaks isospin symmetry. However, also here a resonance could exist, but would be even more unstable; see the experimental study in Refs. [59,60] and theoretical discussion in Ref. [61].

In conclusion, in the present work we have found that a pole on the second Riemann sheet in the S-wave $I = 1$ channel is present. As discussed in Refs. [1,10,12,35] one does not need to include an explicit degree of freedom in the Lagrangian, since a quartic interaction together with its resummation would mimic the effect of a propagator in the S wave. Within this context, it would be very interesting if the position of the pole could be also investigated in the context of such effective approaches.

Turning back to neutron-proton scattering studied in this work, the next step has been the inclusion of the resonance $f_0(500)$: a remarkably good agreement with SAID results is obtained when only the dibaryon and the resonance $f_0(500)$ are considered (Fig. 5). These results show that these two resonances are most important for the description of the SAID results.

Switching on the other mesons causes a disagreement at large momenta, because the contribution of the pions is too large without introducing a form factor to suppress large momenta. Moreover, also the differential cross sections cannot be reproduced (Fig. 6). This mismatch can, however, be removed by including a form factor. One then obtains a good description of SAID results at high momenta (Fig. 7). Also in this case, the role of $f_0(500)$ is important: by switching it off, the shape of the differential cross section is qualitatively wrong.

As an outlook for future studies, one could use our chiral approach to study reactions in which mesons are produced, such as $NN \to NNX$ with $X = \omega, \rho, \ldots$ (see Ref. [62] for a preliminary investigation). These reactions are at the center of experimental studies (see, e.g., Ref. [63]), and their investigation is important in hadronic physics. Also similar reactions involving strangeness are relevant: for that purpose one would need the full version of the eLSM for $N_f = 3$, including baryons (a first step towards this goal has been performed in Ref. [25]) as well as the full nonet of light-scalar mesons below 1 GeV. For instance, the reaction $pp \to ppK$ has received considerable attention [64]. The determination of the baryon-baryon-meson couplings in the three-flavor case is not only relevant for hadron vacuum physics but also in the context of neutron-star investigations [65].

ACKNOWLEDGMENTS

The authors would like to thank S. Gallas, A. Habersetzer, L. Olbrich, D. Parganlija, and M. Zetenyi for their help during this work. Special thanks go to S. Leupold, J. Reinhardt, and J. Schaffner-Bielich for very helpful suggestions and to O. Mattelaer for his support in running and debugging MadGraph. We would also like to thank H. Feldmeier, J. Gegelia, J. Haidenbauer, and H.-W. Hammer for useful discussions. This work was supported by DFG Grant No. RI 1181/6-1.

[1] R. Machleidt, K. Holinde, and Ch. Elster, Phys. Rep. **149**, 1 (1987).
[2] D. B. Kaplan, Nucl. Phys. B **494**, 471 (1997).
[3] D. B. Kaplan, M. J. Savage, and M. B. Wise, Phys. Lett. B **424**, 390 (1998).
[4] D. B. Kaplan, M. J. Savage, and M. B. Wise, Nucl. Phys. B **534**, 329 (1998).
[5] J. W. Chen, G. Rupak, and M. J. Savage, Nucl. Phys. A **653**, 386 (1999).
[6] X. Kong and F. Ravndal, Phys. Lett. B **450**, 320 (1999).
[7] J. Gegelia, Eur. Phys. J. A **19**, 355 (2004); Phys. Lett. B **463**, 133 (1999); **429**, 227 (1998).
[8] E. Epelbaum, Prog. Part. Nucl. Phys. **57**, 654 (2006).
[9] E. Epelbaum, H. W. Hammer, and U. G. Meissner, Rev. Mod. Phys. **81**, 1773 (2009).
[10] U. van Kolck, Prog. Part. Nucl. Phys. **43**, 337 (1999).
[11] P. F. Bedaque and U. van Kolck, Annu. Rev. Nucl. Part. Sci. **52**, 339 (2002).
[12] L. Coraggio, A. Covello, A. Gargano, N. Itaco, D. R. Entem, T. T. S. Kuo, and R. Machleidt, Phys. Rev. C **75**, 024311 (2007).
[13] D. R. Entem, N. Kaiser, R. Machleidt, and Y. Nosyk, Phys. Rev. C **92**, 064001 (2015).
[14] J. Gasser and H. Leutwyler, Ann. Phys. (NY) **158**, 142 (1984). See also S. Scherer, Adv. Nucl. Phys. **27**, 277 (2003) and references therein.
[15] A. W. Thomas and W. Weise, *The Structure of the Nucleon* (Wiley, Berlin, 2001).
[16] B. W. Lee, *Chiral Dynamics* (Gordon and Breach, New York, 1972).
[17] V. Koch, arXiv:nucl-th/9512029.
[18] S. Gasiorowicz and D. A. Geffen, Rev. Mod. Phys. **41**, 531 (1969); P. Ko and S. Rudaz, Phys. Rev. D **50**, 6877 (1994); M. Urban, M. Buballa, and J. Wambach, Nucl. Phys. A **697**, 338 (2002).
[19] D. Parganlija, F. Giacosa, and D. H. Rischke, Phys. Rev. D **82**, 054024 (2010).
[20] S. Janowski, D. Parganlija, F. Giacosa, and D. H. Rischke, Phys. Rev. D **84**, 054007 (2011).
[21] D. Parganlija, P. Kovacs, G. Wolf, F. Giacosa, and D. H. Rischke, Phys. Rev. D **87**, 014011 (2013).
[22] S. Janowski, F. Giacosa, and D. H. Rischke, Phys. Rev. D **90**, 114005 (2014).
[23] S. Gallas, F. Giacosa, and D. H. Rischke, Phys. Rev. D **82**, 014004 (2010).
[24] S. Gallas and F. Giacosa, Int. J. Mod. Phys. A **29**, 1450098 (2014).
[25] L. Olbrich, M. Zétényi, F. Giacosa, and D. H. Rischke, Phys. Rev. D **93**, 034021 (2016).
[26] C. DeTar and T. Kunihiro, Phys. Rev. D **39**, 2805 (1989).
[27] D. Zschiesche, L. Tolos, J. Schaffner-Bielich, and R. D. Pisarski, Phys. Rev. C **75**, 055202 (2007).
[28] D. Jido, M. Oka, and A. Hosaka, Prog. Theor. Phys. **106**, 873 (2001); D. Jido, Y. Nemoto, M. Oka, and A. Hosaka, Nucl. Phys. A **671**, 471 (2000); A. Hosaka, D. Jido, and M. Oka, Prog. Theor. Phys. Suppl. **149**, 203 (2003).
[29] S. Godfrey and N. Isgur, Phys. Rev. D **32**, 189 (1985). See also the summary of the "quark model" in Ref. [38].
[30] E. van Beveren, T. A. Rijken, K. Metzger, C. Dullemond, G. Rupp, and J. E. Ribeiro, Z. Phys. C **30**, 615 (1986); E. van Beveren, D. V. Bugg, F. Kleefeld, and G. Rupp, Phys. Lett. B **641**, 265 (2006); J. R. Pelaez, *ibid.* **92**, 102001 (2004); J. A. Oller and E. Oset, Nucl. Phys. A **620**, 438 (1997); **652**, 407 (1999); J. A. Oller, E. Oset, and J. R. Pelaez, Phys. Rev. D **59**, 074001 (1999); **60**, 099906 (1999).
[31] A. H. Fariborz, R. Jora, and J. Schechter, Phys. Rev. D **72**, 034001 (2005); A. H. Fariborz, Int. J. Mod. Phys. A **19**, 2095 (2004); M. Napsuciale and S. Rodriguez, Phys. Rev. D **70**, 094043 (2004); L. Maiani, F. Piccinini, A. D. Polosa, and V. Riquer, Phys. Rev. Lett. **93**, 212002 (2004); F. Giacosa, Phys. Rev. D **74**, 014028 (2006); F. Giacosa and G. Pagliara, Nucl. Phys. A **833**, 138 (2010).
[32] J. R. Pelaez, arXiv:1510.00653.
[33] S. Gallas, F. Giacosa, and G. Pagliara, Nucl. Phys. A **872**, 13 (2011).
[34] A. Heinz, F. Giacosa, and D. H. Rischke, Nucl. Phys. A **933**, 34 (2015).
[35] R. Machleidt, Phys. Rev. C **63**, 024001 (2001).
[36] CNS Data Analysis Center, database SAID, George Washington University (NP, current solution) http://gwdac.phys.gwu.edu/.
[37] W. I. Eshraim, F. Giacosa, and D. H. Rischke, Eur. Phys. J. A **51**, 112 (2015).
[38] K. A. Olive *et al.* (Particle Data Group), Chin. Phys. C **38**, 090001 (2004).
[39] V. Dmitrasinovic and F. Myhrer, Phys. Rev. C **61**, 025205 (2000).
[40] F. Giacosa, Phys. Rev. D **75**, 054007 (2007).
[41] T. Wolkanowski, F. Giacosa, and D. H. Rischke, Phys. Rev. D **93**, 014002 (2016).
[42] T. Wolkanowski, M. Soltysiak, and F. Giacosa, Nucl. Phys. B **909**, 418 (2016).
[43] T. T. Takahashi and T. Kunihiro, Phys. Rev. D **78**, 011503 (2008).
[44] A. Heinz, S. Struber, F. Giacosa, and D. H. Rischke, Phys. Rev. D **79**, 037502 (2009).
[45] C. Amsler and F. E. Close, Phys. Rev. D **53**, 295 (1996).
[46] Y. B. Dong, A. Faessler, T. Gutsche, and V. E. Lyubovitskij, Phys. Rev. C **78**, 035205 (2008).
[47] A. Faessler, T. Gutsche, M. A. Ivanov, V. E. Lyubovitskij, and P. Wang, Phys. Rev. D **68**, 014011 (2003).
[48] L. P. Kaptari and B. Kampfer, Nucl. Phys. A **764**, 338 (2006).
[49] M. L. Goldberger, M. T. Grisaru, S. W. MacDowell, and D. Y. Wong, Phys. Rev. **120**, 2250 (1960).
[50] A. Alloul *et al.*, Comput. Phys. Commun. **185**, 2250 (2014).
[51] J. Alwall *et al.*, J. High Energy Phys. 07 (2014) 079.
[52] F. Giacosa and G. Pagliara, Phys. Rev. C **76**, 065204 (2007).
[53] A. N. Ivanov, M. Cargnelli, M. Faber, H. Fuhrmann, V. A. Ivanova, J. Marton, N. I. Troitskaya, and J. Zmeskal, arXiv:nucl-th/0407079.
[54] S. B. Borzakov, N. A. Gundorin, and Y. N. Pokotilovski, Phys. Part. Nucl. Lett. **12**, 536 (2015).
[55] A. Spyrou *et al.*, Phys. Rev. Lett. **108**, 102501 (2012).
[56] H. W. Hammer and S. König, Phys. Lett. B **736**, 208 (2014).
[57] J. MacDonald and D. J. Mullan, Phys. Rev. D **80**, 043507 (2009).
[58] K. Kisamori *et al.*, Phys. Rev. Lett. **116**, 052501 (2016).
[59] J. Gomez del Campo *et al.*, Phys. Rev. Lett. **86**, 43 (2001).
[60] S. Dymov *et al.*, Phys. Rev. C **81**, 044001 (2010).
[61] J. Haidenbauer and Yu. N. Uzikov, Phys. Lett. B **562**, 227 (2003).

[62] K. Teilab, F. Giacosa, and D. H. Rischke, Acta Phys. Pol. Suppl. **7**, 487 (2014).

[63] F. Balestra *et al.* (DISTO Collaboration), Phys. Rev. C **63**, 024004 (2001); **69**, 064003 (2004).

[64] T. Rozek *et al.*, Phys. Lett. B **643**, 251 (2006); Y. Valdau *et al.*, Phys. Rev. C **81**, 045208 (2010); A. Budzanowski *et al.*, Phys. Lett. B **692**, 10 (2010); G. Agakishiev *et al.*, Phys. Rev. C **85**, 035203 (2012).

[65] S. Weissenborn, D. Chatterjee, and J. Schaffner-Bielich, Nucl. Phys. A **881**, 62 (2012); A. Drago, A. Lavagno, G. Pagliara, and D. Pigato, Phys. Rev. C **90**, 065809 (2014).